Biomass and Bioenergy 190 (2024) 107390

Contents lists available at ScienceDirect

Biomass and Bioenergy

journal homepage: www.elsevier.com/locate/biombioe

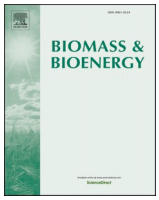

Gasification of mixed plastic-biomass pellets in an updraft fixed bed reactor: A simplified dynamic model

Antonio Tripodi, Ilaria Prada, Matteo Tommasi, Ilenia Rossetti *

Chemical Plants and Industrial Chemistry Group, Dip. Chimica, Università Degli Studi di Milano, CNR-SCITEC and INSTM Unit Milano-Università, Via C. Golgi 19, 20133, Milan, Italy

ARTICLE INFO

Keywords:
Biomass
Plastic
Pyrolysis
Process simulation
Waste recycle
Gasification

ABSTRACT

In the context of materials recycling, updraft gasifiers are promising small and middle-scale reactors to obtain building blocks and/or energy from waste plastic and biomasses. To this aim, these kinds of materials can also be mixed and reduced into pellets, while the needed heat enters the process with a heated carrier gas. In order to preliminarily design a gasifier to check its feasibility with an available feedstock, currently available models are inadequate. Thermodynamic ones are useless for the purposes of sizing, while too detailed rate-based models (e.g. based on fluid-dynamic modelling) are too substrate specific, need detailed input data and are extremely time consuming. A dynamic model of a fixed-bed reactor for biomass gasification is presented here. The gasifier is loaded continuously from the top with solid pellets and fed with counter-current air flow. The model considers: i) a one-step gasification kinetics, yielding a product spectrum which matches experimental data from the literature; ii) dynamic gas and solid energy balances and iii) steady-state energy balance for the furnace. The model has been applied to describe a tubular furnace (Ø 40 cm) which gasifies 500–1000 kg day^{-1} of mixed wastes using air heated up to 1200 °C: on the basis of the produced chemicals, the energy consumption was estimated as ca. 2 MJ per kg of solid feedstock. This simplified approach proved robust in describing the overall yields and start-up dynamics, showing higher reliability than equilibrium models in addressing the temperature profiles, at the cost of a simplified reaction kinetic and pellet description with respect to more complex simulation models. The model validation was done by comparison between the calculations results and available pilot-plant data. An overall good fit of the data can be concluded. The solid-gas heat transfer and the bed packing are the main computational criticalities to achieve a reliable process description.

1. Introduction

Worldwide, the amount plastic waste has doubled with respect to two decades ago and most of it still ends up in landfill, incinerated or dispersed into the environment. The amount that is successfully recycled, according to a recent OECD report is only 9 % [1]. Half of all plastic waste is produced in OECD countries, e.g. in average 221 kg per person in the USA and 114 kg per person in the EU.

Plastic and biomass-based materials are widespread both as feedstock and finished products, but can lead to a significant environmental impact (either as a pollutant when dispersed improperly in the environment or from the point of view exploitation of resources) if disposal is their only end-of-life option. The so-called transition from 'linear' to 'circular' material processing relies on the minimisation of raw sources, the increase of products lifetimes and the recovery/recycling of wastes prior to their final disposal [2]. Global waste management guidelines consider: primary recycling (essentially a re-use), secondary recycling (e.g. turning a plastic object into a different plastic item, with some limitations on the final applications and deterioration of the properties and value of the object), tertiary recycling (break-down the waste into chemicals that can be used as building-blocks) and quaternary recycling, i.e. conversion into energy [3,4].

Most plastics are virgin, freshly made on demand from crude oil or gas, which also raises concerns on the availability and critical dependence on these feedstocks. Global production from recycled plastics has grown from 6.8 million tonnes in 2000 to 29.1 in 2019, but this is still only 6 % of the size of total plastics production. Tertiary recycling is becoming more and more attractive, since regenerating building blocks can give a truly new life to wastes, not only plastic ones, but more in general urban wastes and waste biomass. The gasification and pyrolysis

* Corresponding author.
E-mail address: ilenia.rossetti@unimi.it (I. Rossetti).

https://doi.org/10.1016/j.biombioe.2024.107390
Received 23 August 2023; Received in revised form 2 August 2024; Accepted 19 September 2024

processes are growing rapidly to maturity, although some technical issues need still to be solved. These include challenges related to operational and investment expenses, high energy usage and upscaling difficulties in commercialization, thus hampering the widespread adoption and implementation of biomass gasification, despite their great potential. Even wider are the points of attention for pyrolysis. The composition and properties of biomass feedstock can vary widely, leading to challenges in achieving consistent and predictable pyrolysis performance. Efficient heat transfer is crucial for achieving high pyrolysis yields, impacting the overall efficiency and economics of the process. Controlling the distribution and quality of the pyrolysis products (biochar, bio-oil and syngas) is critical and designing and scaling up pyrolysis reactors to industrial scale while maintaining process efficiency and product quality poses technical challenges. Reactor design plays a crucial role in determining the overall performance of the pyrolysis process. Improving the energy efficiency of biomass pyrolysis processes is essential for reducing operational costs and environmental impacts: enhancing energy recovery and minimizing energy losses during the process are key technical considerations. Finally, managing contaminants such as ash, tar, and alkali metals during biomass pyrolysis is crucial to prevent equipment fouling and maintain product quality.

Furthermore, the relatively small size of plants introduce challenges for their economic sustainability. From a technical point of view, gasification and pyrolysis differ essentially for the required temperature and the presence of oxygen, but both can be successfully applied to different waste typologies.

Plastic and biomass wastes, besides their chemical affinity, present mechanical properties that allow to mix them into a feedstock for combustion or gasification [5]. Gasification is a process in which various kinds of biomasses can be converted to syngas, tar and a solid residue called char, in different proportions, using a gasifying agent (e.g. oxygen, air or steam). Various types of gasifiers have been proposed: fixed (moving) bed, fluidised bed and entrained flow gasifiers. Each of them holds pros and cons and may be suitable or not for a given application. In particular, fixed bed reactors are the oldest and most well assessed ones and are further classified in updraft (counter-current), downdraft (co-current) and cross-flow, depending on the relative direction of the solid and fluid feeds. Fixed bed gasifiers are the most commercially equipped systems because of simple design and easy operation [6,7]. They are suitable for small scale applications and are the most used for decentralised power generation from biomass [8]. Updraft gasifiers in particular have high thermal efficiency, small pressure drop and slight tendency to slag formation. These are also suitable for applications where small dust amount is acceptable in the product gas and can handle biomass with high moisture and ash content. Shortcomings are the longer start up times, higher tar yields with respect to other options [8]. They are suitable to small-middle scale designs, generally up to 10 MW [6]. Downdraft configurations are used when lower tar yield is desired, though with lower thermal efficiency [9].

In this context, computational methods have widened their scope from the strictly thermal and mechanical design of the furnaces and reactors, to the evaluation of the chemical and energy yields, becoming indispensable predictive tools for the early stages of process design. Indeed, a basic question is whether a given waste pool may be suitable for valorisation as regenerated chemicals (e.g. for the production of syngas or regenerated olefin monomers) and if a plant of a given scale can be technically and economically feasible. This is important to address the fate of a pure or mixed waste and to suggest to policy-makers or companies how to exploit it successfully and remuneratively. At the level of preliminary design, simplified models are needed to have a reasonable estimate on the feasibility of a process, without incurring in the use of too sophisticated models. The latter require huge efforts and time in calculations which is not available at the very preliminary stage of feasibility estimate. Furthermore, rigorous models require very detailed input data on the feedstock, which are often not available and not fastly collectable. Currently available models are either purely thermodynamic (equilibrium based), or kinetic-based models.

Thermodynamic models are very useful to fix overall process conditions, or to represent in a rather simple way available data (after a proper tuning of the embedded degrees of freedom), or focusing on heat integration in the context of larger plants. For example, Chmielniak et al. [10]resorted to actual plant data to fix thermal balances with a shortcut brute-formula approach. Kanna et al. [11] developed a reaction network for gas-phase reaction simplifying the volatilisation step. Cohce et al. [12] adopted a unique reaction step to build a complex downstream heat integration network, whereas Aghaalikhani and co-workers [13] skipped the reaction kinetics description to focus on the hydraulics and fluid-dynamics of a fluidised-bed reactor. However, these models do not allow fully reliable predictions and equipment design, which are made possible by kinetic models only. Therefore, thermodynamic models are unsuitable for sizing (even preliminary) and thus they cannot be used for costing. Therefore they do not allow to answer the question whether a process for biomass valorisation of a given size is feasible or not.

On the other hand, kinetic models are more complex by definition and introduce simulation issues. For instance they couple chemical and mechanical phenomena, so they cover actually a wide range of assumptions, mathematical refinements and are treated with widely different software. To introduce some examples, Eikeland et al. [14] used Aspen Plus© to compare different kinetic and equilibrium models results. Martínez-Lera and Pallarés Ranz [15] coupled reaction kinetics and semi-empirical treatment of a fluidised bed void fraction profile. Goyal and Pepiot [16] resorted to a full Computational Fluid Dynamic (CFD) approach, as well as Patra et al. and Di Blasi [17,18]. Nemtsov and Zabaniotou [19] built a complex kinetic and hydraulic model with an inside-out approach, starting from the description of the solid particles. Specifically referring to updraft gasifiers, kinetic models have been developed by Qi et al. [20] and by Cerinski et al. [21].

These models are very tightly related to the specific feedstock and application, and they are intrinsically very complex and computationally demanding. Their use is needed of course to get reliable and precise sizing of reactors for the valorisation of waste mixtures to produce fuels and chemicals. Nevertheless, preliminary estimates mostly aim to address the basic economic viability of the solution, for which a very rough estimate of equipment sizing is only needed, impossible or fully unreliable when done through equilibrium models and too time consuming and substrate-dependent if one uses kinetic models.

To fill the gap between equilibrium-based models and very detailed kinetic or CFD approaches, the scope of the present work is to develop and validate a simplified kinetic model for the gasification of a mixed feedstock constituted of plastic plus biomass. An updraft cylindrical furnace loaded top-down with the solid has been selected as reactor. This type of reactor has been given much attention in the previously mentioned literature, and promises to be the best suited for middle-scale plants treating already pelletised fuels. To our best knowledge, a simplified kinetic approach is not available for this field, and it would be enormously useful to estimate the feasibility of biomass and plastic waste valorisation plants. This would allow considerable time saving with respect to more complex kinetic models, together with more reliable estimates of energy/material balances and costing with respect to thermodynamic models.

Furthermore, rigorous models and examples from the literature often refer to a pure substrate, while in real applications a mixed waste feedstock is usually treated. In this manuscript, a step by step protocol is proposed to retrieve approximate estimates of the relevant mixture properties to be used in the simplified model. This procedure, detailed for this specific case, is easily extendable to other mixed substrates for this application or different ones.

Although the presented simulation is not as detailed as others reviewed, it is able to reproduce the essential features of the process and to identify the computational bottlenecks that, once solved, can increase the calculations reliability without aiming for a comprehensive

mathematical description of all the involved phenomena. This example is useful to provide a general procedure for deriving a lumped simplified approach to preliminarily assess the potential for valorisation of solid waste materials into syngas to regenerate chemicals.

2. Materials and methods

2.1. Feedstock, stoichiometry, properties and kinetic data

The equipment scheme and the product yields are taken from available data [22], in order to validate the model predictions, while the reaction kinetics is derived for comparison with plastics [23–25].

Many articles in the literature take into account single, well characterised materials with kinetics derived on purpose. However, for real applications, mixed wastes are better used, either mixed plastics or biomass feedstocks of different origin and of which only an averaged composition and (just in few cases) apparent kinetics are known.

Therefore, the first scope is to build a procedure to retrieve sufficiently representative compositional analysis and kinetic data, to build a predictive simplified model for preliminary design purposes. To this aim, pilot scale data have been selected, obtained from the gasification of a mixed, not well defined material. The available data were as follows.

According to Ponzio et al. [22], the combustion of Rofire® pellets were simulated. Rofire® is a mixed plastic-biomass fuel obtained by mixing 55 wt% recycled plastics and 45 wt% biomass scrap. Rofire® is a solid fuel derived from paper fiber, fabric fiber, wood chips and plastics. With respect to woody biomass, it has a lower content of fixed carbon, lower oxygen content due to the high amount of plastics and a higher content of ashes and volatiles. The brute formula of this mixed compound is presented in Table 1. It is roughly compared with that of lignin and polyethylene derived from different sources, to have an approximate idea of the positioning of the composition between two opposite possible components.

As stated in Ref. [22], the gasifier is a vertical cylinder with an inner diameter of 0.4 m and included five sections from bottom to top: slag box to collect the molten slag, wind box, grate and pebble bed part, fixed bed of feedstock, producer gas outlet section and feeder section from top.

These data were used to validate the model. The products spectrum was taken from Ref. [22] as summarised in Table 2. The produced gas was analysed with respect to composition, including a detailed characterization of the tar. Lower heating values up to 9.5 MJ/Nm^3 and gas yields as high as 3.4 Nm^3/kg were achieved. The composition (in general reported on a dry basis) of the tars, suggested extensive cracking as a result of the high temperatures of the outgoing gas. Although the authors listed several higher-weight molecules as main components of tar, giving their amounts in terms of micrograms per gram of flue gas, for this work only benzene, toluene and anthracene are quantified. This reflects the high cracking efficiency and accounts for the predominant species characterised in the effluent. These three components, in different experiments, accounted for at least 60–70 % of the tar composition, which is in any case a minor fraction. The other detected components are sparse and ca. one order of magnitude less abundant. One exception is xylene, which however was found to strongly vary in concentration under different conditions, being often a minor component.

As for the reaction kinetics many experimental papers have been reviewed. Some of them are summarised in Table 3, which includes the heating rate, one of the significant variables in thermal analyses to retrieve such data, and the estimated kinetic parameters. More details on the experimental procedure to quantify kinetics are reported in the cited references and in the bibliography reported therein [23–25].

As seen above, Rofire® is a complex material and it has been selected here on purpose. Most simulation and modelling papers deal with well characterised substrates and detailed kinetics of pure compounds (e.g. pure polyethylene, PE), which is not usually the case of real waste feedstocks, where mixed materials are usually present. By comparing the retrieved kinetics reported in Table 3, the kinetic parameters of polyethylene were used to simulate the reactor, since the exact composition of the matrix was not known. Given the higher activation energy, this choice can be considered as conservative for preliminary sizing or rating. Furthermore, polyethylene is the most abundant plastic waste, presumably the predominant fraction of the plastic content in the selected material.

The solid pellets were modeled as spheres with a Gaussian-distributed size (average diameter: 6 mm, standard deviation: 2 mm), though the original shape is pellets. This allowed modelling of the heat transfer across the particle and it is better for the further implementation of particle shrinking. Other parameters relevant for the simulation are collected in Table 4 and compared with similar materials. In particular, the thermal diffusivity (α), the thermal conductivity (k) and the density (ρ).

Being a mixture of plastic waste and biomass, the reagent specific heat is heuristically interpolated as shown in the following Fig. 1 (data are taken from Refs. [28,37–39]). A mixture of amorphous and crystalline PE is considered as representative for the plastics fraction of the "Rofire" reagent, while the cellulose is chosen for representing the "Rofire" biomass fraction.

The specific heat capacities variation with temperature of the cellulose and the completely amorphous and crystalline PE and their

Table 1
Elemental analysis (%) of relevant materials. Lignin data from Ref. [26] and polyethylene (deriving from plastic wastes) data from Ref. [27] are added for comparison.

	'Rofire'	Lignin	Polyethylene
Moisture (%)	2.90		–
Ash (%)	6.00	0.45–4.25	–
Volatile matter (%)	84.4		100
Fixed Carbon (%)	6.70		–
C (%)	66.0	59–66	85.4
H (%)	11.0	5.80–6.40	14.2
N (%)	0.30	0.49–0.67	0.08
O (%)	22.0	25.3–32.0	0.15
Others (%)	0.70	0–2.6	0.17

Table 2
Products yield from Ref. [22] (fractions obtained excluding Nitrogen, dry basis). The reference solid consumption is 44 kg h^{-1}, and 25–30 kg h^{-1} for the simulation of this work.

Product	Yield		Rated flow	
	(Nm^3 kg$_{fuel}^{-1}$)	(%)	(kg h^{-1})	(kmol h^{-1})
N_2	1.85		97.2	3.45
H_2	0.500	32	1.94	$9.69\bullet10^{-1}$
CO	0.473	30	25.7	$9.17\bullet10^{-1}$
CO_2	0.272	17	23.2	$5.27\bullet10^{-1}$
CH_4	0.189	12	5.86	$3.66\bullet10^{-1}$
C_2H_2	0.013	0.8	0.655	$2.52\bullet10^{-2}$
C_2H_4	0.104	6.6	5.64	$2.02\bullet10^{-1}$
C_2H_6	0.002	<1	0.116	$3.88\bullet10^{-3}$
C_3H_8	0.015	1.0	1.28	$2.91\bullet10^{-2}$
C_6H_6	–		0.984	$1.26\bullet10^{-2}$
C_7H_8	–		0.194	$2.11\bullet10^{-3}$
$C_{10}H_8$	–		0.482	$3.77\bullet10^{-3}$

Table 3
Kinetic data of several polymers and cellulose.

Material	Ea (kJ mol^{-1})	Duration (h)	T_{ramp} (K min^{-1})	Ref.
PE	235	$1.86\bullet10^{-6}$	10	[23]
PP	224	$6.20\bullet10^{-7}$	5-10-20-40	[24]
PVC	185	$1.25\bullet10^{-8}$	10	[23]
PS	219	$3.76\bullet10^{-7}$	10	[23]
cellulose	181	$1.15\bullet10^{-8}$	5-10-15	[25]

Table 4
Relevant properties of 'Rofire' and other materials. The brute formulas are normalised to 1 carbon atom.

Material	Formula	PM	α	k	ρ (@ 25 °C)	Ref.
		(g mol^{-1})	(m^2 s^{-1})	(W m^{-1} K^{-1})	(kg dm^{-3})	
PE	CH_2	14	2.2•10^{-7}	0.3–0.5	0.92–0.97	[28–30]
PP	CH_2	14	9.6•10^{-8}	0.11–0.22	0.85–0.94	[31–33]
PS	CH	13	1.8•10^{-8}		0.96–1.05	[33,34]
Wood	$CH_{1.2}O_{0.4}$	20	1.5–3.0•10^{-7}	0.1–0.2	0.20–0.70	[26,35,36]
Rofire	$CH_2O_{0.25}$	18	1.0•10^{-7}		0.47	

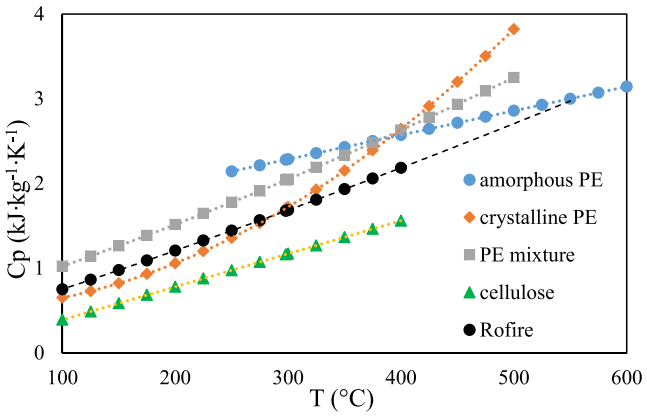

Fig. 1. Specific heats interpolation [28,37–39].

mixture are shown in Fig. 1.

The PE specific heat capacities in kJ kg^{-1} K^{-1} are obtained from the data on molar basis of Gaur et al. [31], by dividing for the molecular weight of the PE repeating unit (-CH_2-). So, the specific heat capacity of a 50:50 mixture of cellulose and PE is considered for representing the whole "Rofire" reagent. The data are interpolated with polynomial curves $c_p = a + bT + cT^2$ as in Table 5.

2.2. Reactor model

The simulation scheme is represented graphically in Fig. 2. The mass, momentum and energy balances for the solid, gas and reactor walls were treated as follows.

a) Gasification stoichiometry was derived from Tables 2 and is (on a mass basis):

$$ROFIRE + 0.512\ O_2 \rightarrow 4.199\times10^{-2}\ H_2 + 0.0040\ N_2 + 0.131 CH_4 + 0.125\ C_2H_4 + 0.0148 C_2H_2 + 0.00256 C_2H_6 + 0.0268\ C_3H_8 + 0.0255\ C_6H_6 + 0.00467\ C_7H_8 + 0.0109\ C_{10}H_8 + 0.613\ CO + 0.436\ CO_2 + 0.0720\ H_2O$$

b) Gasification kinetics was computed according to the Arrhenius model with respect to the normalised solid mass w. The activation energy was taken in the range of Table 3. The prefactor and the reaction order were estimated interpolating the data published by Meng et al. [23].

$$\frac{-dw}{dt} = 4.0\times10^{11} s^{-1} \times e^{-\left(\frac{E_a}{RT}\right)} \times w^{0.95} \quad (1)$$

Table 5
Specific heat capacities coefficients of the cellulose, the amorphous and crystalline PE, a mixture of them and the "Rofire" reagent.

Data	a (kJ kg^{-1} K^{-1})	b (kJ kg^{-1} K^{-2})	c (kJ kg^{-1} K^{-3})
Amorphous PE	1.429	2.857•10^{-3}	/
Crystalline PE	5.000•10^{-1}	2.143•10^{-4}	1.286•10^{-5}
PE mixture	5.714•10^{-1}	4.286•10^{-3}	2.143•10^{-6}
Cellulose	6.468•10^{-16}	3.900•10^{-3}	/
Rofire	3.157•10^{-1}	4.243•10^{-3}	1.071•10^{-6}

c) The solid spheres were heated by the gas according to the analytical solution of the partial-derivative heat dynamic equation:

$$\Theta(t,r) = \Phi(r) e^{-\left(\alpha\times\frac{t}{r^2}\right)} \quad (2)$$

where:

$$\Theta(t,r) = \frac{T_{ext} - T(r,t)}{T_{ext} - T(r,0)} \quad (3)$$

and $\Phi(r)$ did not depend on time. This means that the skin and average temperatures follow the same transients, and can be represented as functions of the Biot number

$$\mathrm{Bi} = \frac{h r_p}{k}$$

by the correlation shown in Fig. 3. The solid enthalpy content was described by the average temperature, while the reaction temperature was taken as the skin one.

This approach of simulating the fuel on a micro-scale with a continuous space definition, and the reactor on a macro-scale with a space discretisation has already been adopted by Ranzi et al. [40], but in this work the solid spheres temperature is given directly by an algebraic equation (rather than a differential one) that relies on the analytical dynamic solution.

k and h in the Bi number are respectively the thermal conductivity of the reagent and the air convective heat transfer coefficient, while r_p is the radius of the reagent sphere (6.21 10^{-3} m). The latter was calculated from the pellet size with equivalent volume.

The thermal conductivity was calculated assuming a heat capacity from literature [28,31,38,39] and a thermal diffusivity coefficient tentatively assumed to be equal to 1 10^{-7} m^2 s^{-1} [34,41]. On the other hand, considering the air forced convection regime into the reactor, one can assume that hair is not less than 10 W m^{-2} K^{-1} [42]. So, the

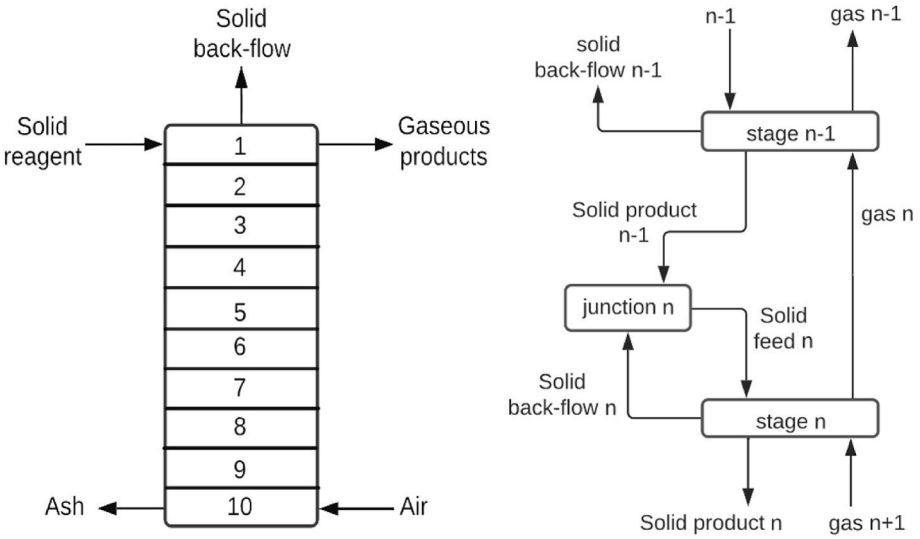

Fig. 2. (Left) multi-layers simulation scheme for the pilot-scale furnace. Each stage was assumed in perfect mixing conditions; (right) detail of the flows connection for each simulation stage.

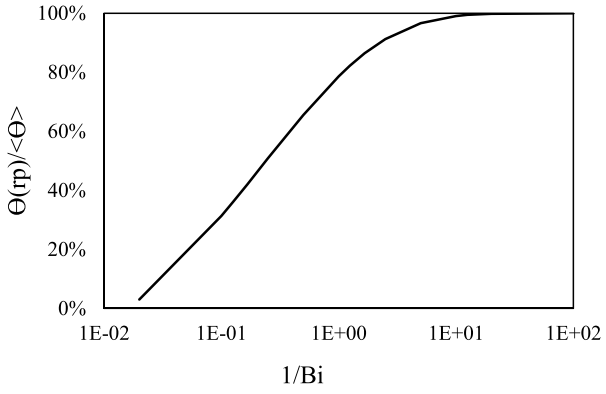

Fig. 3. Correlation between the skin and average temperature for a solid sphere, according to the environmental heat exchange conditions represented by the Biot number.

Table 6
Calculation of 'Rofire' enthalpy of formation. The HHV is taken as negative for an exothermic reaction.

	m	HHV	$\Delta_f H°$	m × $\Delta_f H°$
	(kg)	(kJ kg^{-1})	(kJ g^{-1})	(kJ)
Rofire	1.00	−29030.5		−8332.76
O_2	2.41	–	0	0
CO_2	2.42	–	−8.943	−21642.1
H_2O	0.99	–	−15.88	−15721.2

calculated Biot number was Bi = 0.66 and 1/Bi = 1.52.

At such value $\Phi(r_p)/\Phi(r = 0) = 73$ % and $\Phi(r_p)/(<\Phi>) = 86$ %, so, for simplicity, in the following calculation the form of Φ was neglected and the Gurney-Lurie chart for the time-dependent solution at the sphere center was used to represent the temperature trend in time in the whole solid.

d) The enthalpy of formation $\Delta_f H°$ of the pellets was calculated after the brute formula and the higher heating value (HHV) reported in Ref. [22] considering the complete combustion of a unitary amount of fuel (data in Table 6): $CH_2O_{0.25} + 1.375O_2 \rightarrow H_2O + CO_2$.

The specific heat was modeled by a polynomial expansion fitting the data in Fig. 1. The reaction heat was calculated once the formation enthalpy of 'Rofire' was known.

The gas-solid heat transfer was given by:

$$q_{gas-solid} = \sum_j A_{s,j}\left(T_g - T_{surf}\right)h_{gas-solid} \tag{4}$$

$$h_{gas-solid} = \frac{k_g}{D_{hyd}}\left(0.023\, Re^{0.8}\, Pr^{0.33}\right) \tag{5}$$

The gas-wall heat transfer was given by:

$$q_{gas-wall} = \pi DL\left(T_g - T_1\right)h_{gas-solid} \tag{6}$$

The wall-solid heat transfer was given by:

$$q_{solid-wall} = \pi DL\left(T_{surf} - T_1\right)h_{rad} \tag{7}$$

$$h_{rad} = \zeta\sigma_B\omega\frac{\left(T_{surf}^4 - T_1^4\right)}{\left(T_{surf} - T_1\right)} \tag{8}$$

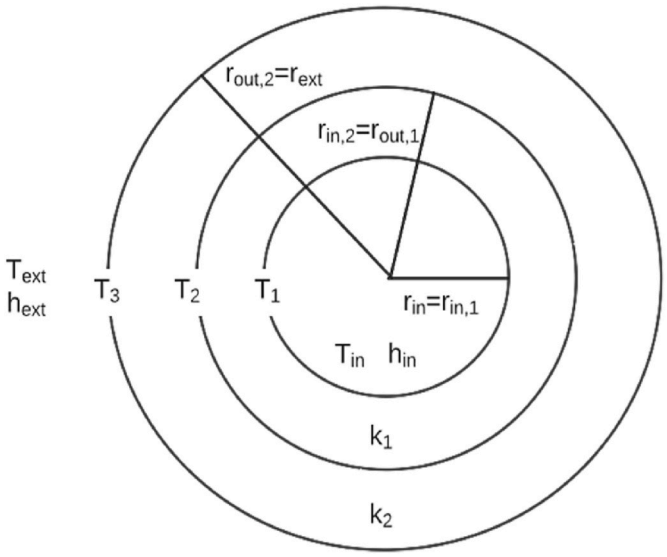

Fig. 4. Top cross-section of the geometrical model for heat dispersion.

The wall-ambient heat transfer was given by (see also Fig. 4):

$$q_{ext} = \pi D_{ext} L (T_3 - T_{ext}) h_{ext} = 2\pi L R_3 \frac{k_2 (T_2 - T_3)}{ln\, r_3/r_2} = 2\pi L R_2 \frac{k_1 (T_1 - T_2)}{ln\, r_2/r_1} \quad (9)$$

e) The overall system energy balance was calculated assuming transient regimes for the gas and the solid, but stationary wall temperatures:

$$\frac{\partial E_g}{\partial t} = F_{g,in} h_{g,in} - F_{g,out} h_g - q_{gas-solid} - q_{gas-wall} \quad (10)$$

$$\frac{\partial E_s}{\partial t} = F_{s,in} h_{s,in} - F_{s,out} h_s - F_{s,back} h_s + q_{gas-solid} - q_{reac} - q_{solid-wall} \quad (11)$$

f) The solid momentum balance was simplified neglecting attrition:

$$\frac{\rho_s}{2}\left(u_s^2 - u_{s,in}^2\right) = 9.81 L (\rho_s - \rho_g) \quad (12)$$

g) The gas momentum balance was calculated via the Ergun formula:

$$1.75 + 150 \frac{1-\varepsilon}{Re} = \frac{F_g}{L\, CV_g} \frac{2\langle r_s \rangle}{u_g^2 \varepsilon^2} \frac{\varepsilon^3}{\rho_g (1-\varepsilon)} \quad (13)$$

$$F_g = CV_g (P_{in} - P) \quad (14)$$

h) Each reactor layer was represented as a perfectly mixed environment. When in each layer the void fraction dropped below a specified threshold, then and upward solid flow was introduced to simulate the furnace filling.

The equations were set-up and solved with Aspen Custom Modeler by Aspen Tech. It is the tool implemented in Aspen Plus simulation package, also in the Dynamics mode, and allows the definition of variables and equations for solving complex and non-standardised modelling problems. Five submodels have been implemented as follows, to represent the above reported equations scheme and its solution mode: 1) Gas convection model; 2) Solid-Reactor wall irradiance model; 3) Reactor wall model; 4) Reactive zone model; 5) Solid particle model.

3. Results and discussion

3.1. Model set up and testing

The model was tested starting with an empty, cold furnace, increasing gradually the solid feed and the air flow and temperatures. The run was organised manipulating the following variables with ramps: a) opening of the furnace bottom, b) gas flow and temperature.

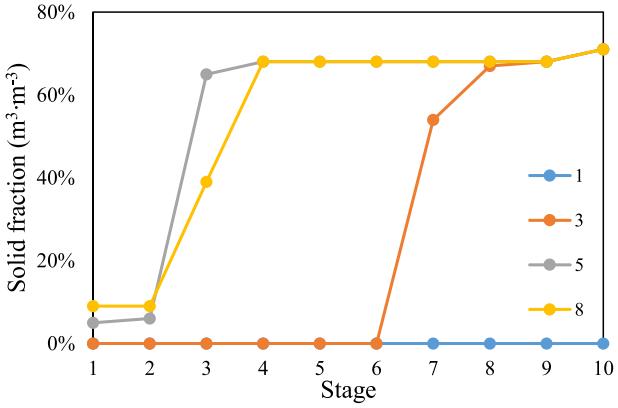

Fig. 5. Reactor filling at different simulation steps (steps '1', '3', '5' and '8').

After each manipulation, the system was let to reach a pseudo-stationary state to evaluate the presence of multiple operating conditions. In total there were 8 relevant condition changes: the first was the furnace bottom closure, the others corresponded to the gas. The time delays between each step and the adoption of ramps instead of step-changes were often necessary. This was due both to physical reasons (the existence of multiple pseudo-steady states, not all relevant) and to mathematical problems (integration convergence, time-discretisation issues) [40].

The bottom stage solid outlet was closed in order to let out 2–3 kg h^{-1} of material (representing ashes) when the void fraction fell below 30 %. Fig. 5 shows the progression of the furnace filling, where the overflow is prevented by the contemporary increase of the combustion rate. The solid mass disappearing from the process results in an increased gas-flow (Fig. 6).

The solid feed was introduced at the 1st stage and as its mass-flow increased, the void fraction of this stage gradually decreased and the reactor started accumulating solid at stages gradually closer to the top one. The reactor was never totally filled thanks to the management of the gas inlet temperature and the solid and gas flowrates. An example of this dynamic behaviour is reported in Fig. 7.

Fig. 8 represents the gas temperatures at different steps (third, fifth and eighth), and Fig. 9 the resulting pellet temperatures. The solid average temperature reached a maximum at the end of the falling zone, where its thermal inertia was low. In the filled zone the material accumulation, together with the reaction duty, tends to 'cool' the pellets with respect to the fixed heat received from the gas. The solid skin temperature, instead, increased steadily with the gas temperature, because it was calculated by the solutions of the conductive balance on the spheres.

This behaviour was determined by three model features.

a) the negative reaction enthalpy determined by the assumed product spectra [40,43], which masked the different contribution of primary and secondary reactions and assigned all the duty to the solid;
b) the constant outflow from the furnace bottom, meant to simulate ashes and tar withdrawal, that let colder pellets from above to lower the average enthalpy content of the bottom stages;
c) the higher difference between skin and gas temperatures (as the gas progressively heated) required a higher difference between skin and average pellet temperatures (as per Fig. 3 solution).

A progressive divarication between center and surface temperature for relatively large (>1 mm) solid particles was found, for low to intermediate contact times, also in the simulations by Gao et al. [44] and Ranzi et al. [40]. Also more sophisticated multi-step models [18] yielded similar solid temperature behaviour, where endothermal reactions

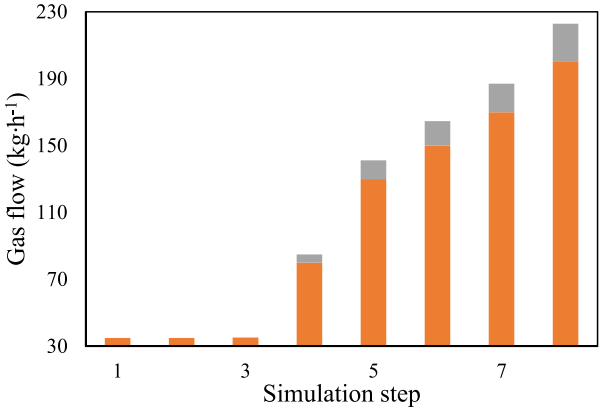

Fig. 6. Gas inlet (orange) and total (orange + grey) flow through the reactor. (For interpretation of the references to colour in this figure legend, the reader is referred to the Web version of this article.)

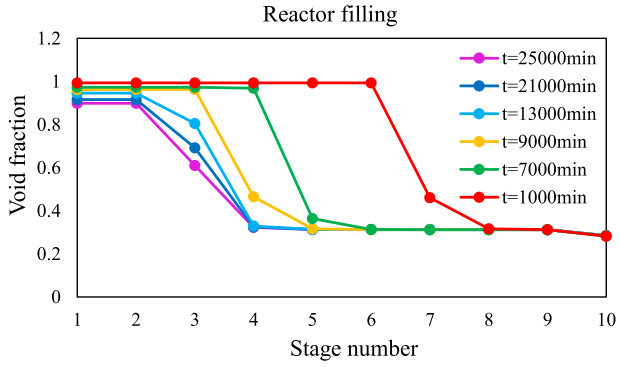

Fig. 7. Example of result of dynamic simulation of reactor filling trough different stages during time.

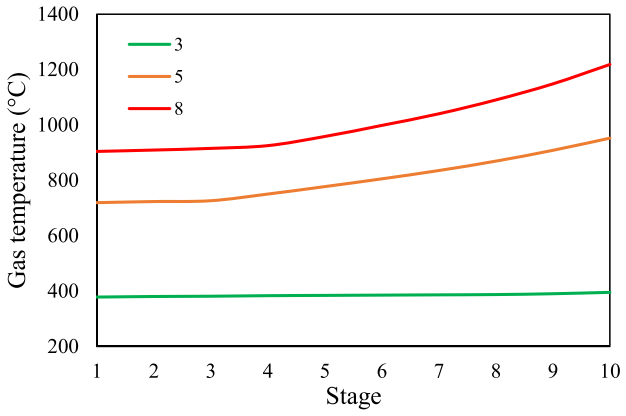

Fig. 8. Gas temperatures along the reactor as the simulation proceeded through steps '3', '5' and '8' as reported in the legend.

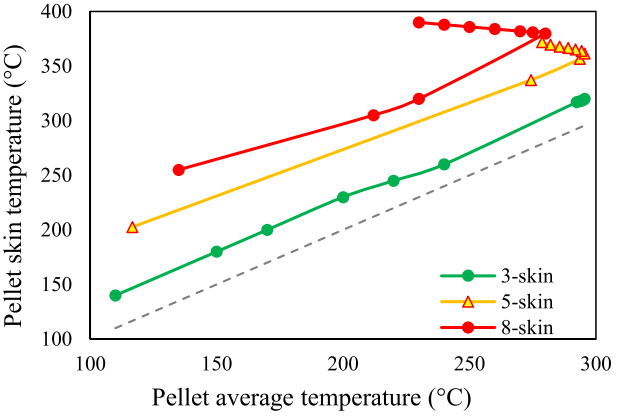

Fig. 9. Pellets skin/average temperatures at the same steps as in Fig. 8 (each marker represents a stage).

prevailed in the bottom zone, while conduction and combustion dominated the top stages.

An indirect evaluation of the global heat input yielded 2.9 MJ kg_{fuel}^{-1}, considering that the heat lost by the carrier gas was roughly: $(1200-900)(°C) \times 1.1\left(kJ\,kg^{-1}\,°C\right) \times 200\left(kg\,h^{-1}\right) = 66\ h^{-1}$ when 23 kg h^{-1} of solid were treated. This basic calculation implies that the products heat can be recovered, otherwise the energy expenditure would increase at least by four times.

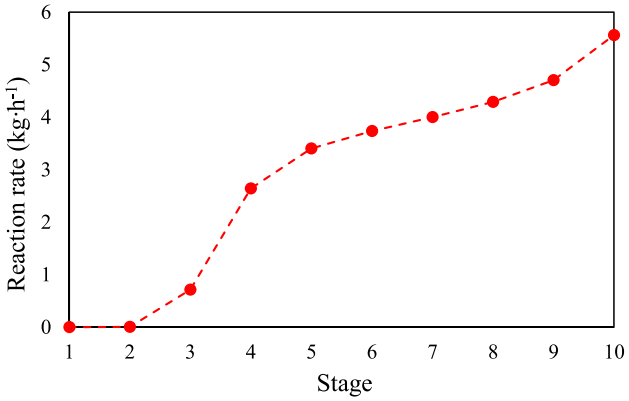

Fig. 10. Reaction rate through the calculation stages at the final pseudo-stationary state.

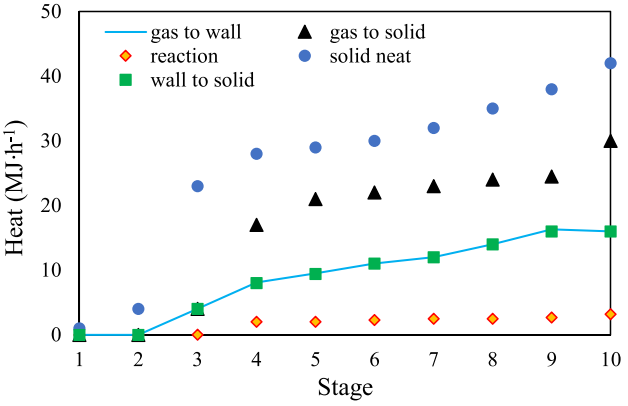

Fig. 11. Heat flows, stage by stage, at the final pseudo-stationary stage.

3.2. Model validation

The overall reaction rate (Fig. 10) followed both the filling trend and the pellet skin temperature trend, and its integral equals the difference between the gas mass flow at the outlet with respect to the inlet. It can be noticed that the reaction started between 370 and 400 °C, in accordance with the reviewed kinetic data. Having neglected fragmentation phenomena, the gasification rate was likely overestimated in the middle stages, while underestimated at the bottom [45].

The heat flows at the final pseudo-stationary stage (Fig. 11) showed that the total heat absorbed by the solid essentially equals the sum of the gas-to-solid heat plus the heat back-radiated from the heated wall, minus the reaction duty. This highlights several important model aspects.

a) the radiant contribution between the gas and the wall was not important, because most of the gaseous stream is in contact with the solid pellets, only, and the exchange with the wall is limited;
b) the convective gas heat transfer coefficient was relatively high, so that the wall temperature (in the filled zone) was close enough to the gas one as to make gas-wall irradiance not important also from this point of view;
c) the wall-solid and gas-wall heat transfer were more or less equal because the different temperature differences were roughly compensated by the different heat transfer coefficients;
d) the back-irradiance from the wall to the solid appreciable decreased the total heat flowing towards the outside: the higher calculated temperature at the insulator surface was 31 °C, in good accordance

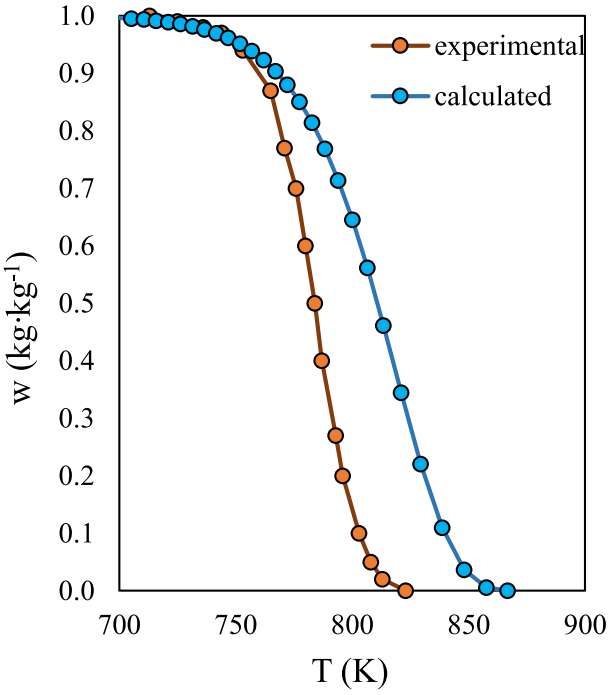

Fig. 12. Comparison of experimental conversion [22] and calculated data through the simplified kinetic model at various temperature.

with good operative practice. Moreover, according to the present calculation the pellets heat balance would be appreciably underestimated without keeping into account this phenomenon.

In comparison with the reference pilot-reactor used as a basis for this work, the air/solid ratio used in the simulation was higher: this is an indirect effect of having neglected the pellet shrinking during combustion.

The kinetic model was compared against experimental data, returning this fit (Fig. 12). The model correctly predicts the trend of substrate conversion, but diverges from data at high temperature.

This required an adjustment of feed composition to correctly represent the trend of conversion and products distribution. The temperatures and duties were reproduced satisfactorily. The model validation against the experimental data used as reference [22] is also reported in Table 7.

Introducing the shrinking of the particles can lead to more accurate prediction of the temperature. However, it must be underlined that the goal of a simplified model is to understand the general feasibility of biomass gasification for a given substrate and the approximate sizing of a possible gasifier for basic economic assessment. Therefore, to this order of magnitude the predictive ability of this model is sufficiently justified.

With respect to recent reports in the literature, the present results represent a good compromise between reliability of the model and manageability. For instance, Cao et al. [46] presented a simulation-based paper involving the gasification of a mixed substrate as in the present case. The simulation of the reactive section was based on steady state assumptions, which are not fully representative of real updraft gasifiers, and includes some stoichiometric and yield reactor models. This is correct when kinetics is not available, but this approach prevents any sizing and costing opportunity. Also Zhou [47] used a mixed simplified approach with yield and Gibbs reactors to simulate the most significant steps of biomass decomposition, while a kinetic approach based on CSTR was used for the reactions involving the produced char. The specific aim was to interpret the energy balances among exo- and endo-thermal reaction steps for the co-production of syngas and char. The results of the model overestimated the yield of H_2, CO and CH_4, while the concentration of CO_2 was underestimated. The largest relative deviation appeared for the methane concentration (58.19 %), because its concentration was much lower than other species. However, compared with the thermodynamic equilibrium model, the prediction error was much smaller.

A very useful collection of kinetic data is reported by Adil et al. [9], where kinetics is considered in CSTR models for the combustion and reduction steps of the gasification process, while the drying and pyrolysis steps are modeled with stoichiometric, yield and Gibbs reactors. Lower errors in the products concentration estimate are reported by the authors with respect to previous works.

In reference to this specific point we should underline that the maximum discrepancy between the calculated and experimental temperature in the presently proposed model was 3.9 %. Indeed, zero residual biomass was achieved at 823 K experimentally while at 857K for the model data. While the calculated biomass conversion of the model was underestimated with respect to the experimental data used for the validation with increasing extent at increasing temperature. A sharper experimental conversion with increasing temperature was observed (Fig. 12) with respect to the calculated profile. For instance, at 793 K, the residual biomass weight was 27 % experimentally, while 72 % calculated and 10 % vs. 59 % at 803 K, respectively.

On the opposite side, very detailed approaches based on CFD simulations are needed to represent fluidised bed reactors. An example is the simulation of soot formation in a cyclone gasifier by Zhao et al. [48]. A complex geometry was considered and fine grid was employed by the authors, achieving a good level of detail in the representation of the products composition. Nevertheless, the calculated data were well in line with the experimental ones regarding CO and CO_2, while the prevision was less satisfactory for H_2 and CH_4. CFD modelling is a fundamental tool also to understand the effect of gasifier geometry and of its components, such as the distribution grids on fluidisation behaviour and on the parameters distribution in the reactor [49]. CFD modelling revealed precious also to simulate and entrained flow gasifier for the conversion of lignin [50]. Also in this case a complex model, coupled with a complex geometry of the reactor was solved including 7 reactions, all of them carefully characterised by the relative kinetic expression and the relative parameters. It is clear that such an approach is not feasible in early design stages. Detailed balance equations and a complex reaction network have been also considered in Ref. [51] for the simulation of the gasification of lignocellulosic biomass. A good correspondence between the model fit and experimental values was acheved at different temperature for H_2, CO and CO_2, while less accurate previsions held for CH_4 and highe hydrocarbons. Finally, the 3D CFD simulation of an updraft gasifier was performed to optimise the yield of syngas in Ref. [52]. Also in this case the yield of syngas was slightly lower than experimental data used for validation, e.g. ca. 35 mol% CO and ca. 30 mol% H_2 experimentally outflowng in comparison to ca. 30 mol% and 25 mol%, respectively, as a result of the model.

Table 7
Comparison for some relevant lump parameters of the reference data and this calculation; the gas yield is taken from experiments where air was used as gasifier instead of steam-air mixtures.

Parameter	Reference Data [22]	This calculation
Outlet gas temperature (°C)	740–930	900
Inlet gas flowrate (kg h^{-1})	125	200
Inlet solid flowrate (kg h^{-1})	44–60	30–40
Inlet gas temperature (°C)	1427–1447	1200
Lowest gas Yield (kg kg^{-1})	1.2	1.0

3.3. Model challenges

The solid phase downflowing experiences an average temperature

reduction, in the bottom stages, that is not explained entirely by the endothermal reactions network adopted, but is imposed by the divarication between skin and core temperatures due the sphere conduction model at relatively high Biot numbers. The fact of subtracting the reaction heat only from the solid phase balance, instead of dividing this contribution between the gas and the solid, also contributes to this computational behaviour.

Keeping relatively large particles leads also to an underestimation of pressure drops, but the calculated values are so low (in the last stage) that this aspect is not problematic.

Having adopted a stationary model for the wall heat dispersion does not play an important role for the process phases description.

The only neglected source of error, in the energy balances, comes from having neglected the gas-wall irradiance in the pellet falling zone, where the gas-wall view factor was appreciable.

The proposed model retains its validity in describing the system hydraulics, and also the interplay between solid accumulation and consumption in the lower stages.

A reliable treatment of the particle shrinking is identified as the main improvement towards better gasification models. Multiple-stage reaction kinetics would lead to more general models, capable of predicting a variety of product yields and reaction heats, but to be checked and tuned against diverse experimental data. A detailed dynamic description of the furnace and of the radiative heat transfer are considered as refinements from the chemical point of view.

However, despite the opportunities for improvements, overall, the level of agreement between computed and experimental data is sufficiently satisfactory for the rough predictive purposes that this model has. It should be recalled that the main aim is to develop a sufficiently manageable tool to understand if the gasification of a mixed waste biomass feedstock may be a valuable substrate and the plant would be economically an option.

4. Conclusions

In this work, a simplified model has been introduced and validated against pilot scale experimental data. A general procedure has been proposed to treat with sufficient reliability and easy manageability, the case of gasifiers treating mixed wastes. While very detailed methods are implemented, e.g. using CFD simulations, in reference to specific gasifiers treating pure compounds, for which accurate thermochemical characterisation data are available, challenges arise when a preliminary feasibility analysis should be done. Indeed, a typical question may arise whether a given waste fraction can be suitable for gasification, with which yield and with what thermal efficiency. In this case, complete dataset with properties of mixed biomass are not available and too complex models are not implementable because too time-consuming and demanding so many unknown parameters to be run.

The present work takes an example of mixed biomass waste to present a general procedure for the estimation of the core parameters of mixed wastes (e.g. specific heat by interpolation, a preliminary estimate of heat transfer coefficients and thermal diffusivity, average stoichiometric formula, etc.). This allows in principle the extension of the same protocol to any type of biomass. Furthermore, a simplified model has been derived, which includes the dynamic loading of the reactor, thermal exchange and heat transfer within the particle and a lumped kinetics. This allows to save time for the preliminary feasibility estimate of realisation of a biomass gasification plant for basic plant design and economics, avoiding the need of detailed kinetic data (unavailable for diversified feedstocks) and products specifications.

With respect to the reference pilot-reactor, the calculated air-to-solid ratio needed to achieve the gasification was higher (5–6 kg kg^{-1} instead of 3) for the present simplified model: this is due to the neglection of the pellet shrinking, with the consequent lower heat transfer rates (solid-side) and lower exchange surface (gas-solid). The estimated temperatures were then 15 % lower in the reactor bottom section, for gas, wall and solid pellets. Comparing the calculated inlet gas heat capacity (280 kJ h^{-1}) with the experimental one (213 kJ h^{-1}), the gas-solid ratio in terms of introduced energy was 2 (the same as achieved by mass balances), indicating that the mismatch between experiments and simulation lies in the heat transfer dynamics, not in the solid flow one. All these (particle shrinking and refinement of heat transfer modelling) are improvements that should allow better refinement of the predictions, though for the general feasibility assessment scope the current level of agreement can already be satisfactory.

Similarly, the simulated reactor filling accounts correctly for the reference bed height, which indicates that the kinetic of plastic pyrolysis is valid for this kind of solid's disintegration. Also supposing, on the other hand, to correct the gas/solid flow ratio resorting to a disintegration kinetics 2 times faster, this would be still in line with the range of documented Arrhenius factors (Table 3). Therefore this simplified model can also stand for preliminary dynamic predictions.

The adopted model calculates an overall pressure drop of 0.02 bar (via the Ergun formula), correctly reproducing the hydraulic behaviour far from fluidisation condition.

Finally, the calculated total heat input for the solid (261 MJ h^{-1}), at a simulated flowrate of 25 kg h^{-1} yields roughly 10 MJ kg^{-1} of specific energy input, of the same order of magnitude of the reported products LHV (i.e. 6 MJ kg^{-1}).

Symbols

A	Area	q	Thermal power
Bi	Biot Number	r	radius
Cv	Equivalent valve coefficient	R	Gas constant
D	Diameter	Re	Reynolds number
E	Internal Energy	T	temperature
Ea	Activation Energy	w	Normalised mass
F	Flow	α	Thermal diffusivity
h	Heat exchange coefficient	ε	Void fraction
ΔH	Enthalpy release	ζ	Emissivity
HHV	Higher Heating Value	ρ	Density
k	conductivity	Θ	Normalised temperature difference
L	Length	σ_B	Stefan-Boltzmann constant
m	mass	Φ	Normalised temperature distribution
PM	Molar Weight	ω	View factor
Pr	Prandtl number		

CRediT authorship contribution statement

Antonio Tripodi: Writing – original draft, Methodology, Formal analysis, Data curation. **Ilaria Prada:** Writing – original draft, Investigation. **Matteo Tommasi:** Visualization, Investigation. **Ilenia Rossetti:** Writing – review & editing, Writing – original draft, Supervision, Resources, Project administration, Methodology, Funding acquisition, Conceptualization.

Data availability

All the data are reported or cited in the manuscript

Acknowledgements

A. Tripodi gratefully acknowledges MUR for funding its RTDA position in the frame of the project Programma Operativo Nazionale "Ricerca e Innovazione" 2014/2020 to deliver research on "Green" topics.

Re-cart Srl, Milan, Italy is gratefully acknowledged for support of this action.

References

[1] www.oecd.org, (n.d.).
[2] L. Fogh Mortensen, I. Tange, Å. Stenmarck, A. Fråne, T. Nielsen, N. Boberg, F. Bauer, Plastics, the circular economy and Europe's environment - a priority for action, European Environment Agency (2021), https://doi.org/10.2800/5847.
[3] C. Block, A. Ephraim, E. Weiss-Hortala, D.P. Minh, A. Nzihou, C. Vandecasteele, Co-Pyrogasification of plastics and biomass, a review, Waste and Biomass Valorization 10 (2019) 483–509, https://doi.org/10.1007/s12649-018-0219-8.
[4] O. Dogu, M. Pelucchi, R. Van de Vijver, P.H.M. Van Steenberge, D.R. D'hooge, A. Cuoci, M. Mehl, A. Frassoldati, T. Faravelli, K.M. Van Geem, The chemistry of chemical recycling of solid plastic waste via pyrolysis and gasification: state-of-the-art, challenges, and future directions, Prog. Energy Combust. Sci. 84 (2021) 100901, https://doi.org/10.1016/j.pecs.2020.100901.
[5] A.K. Singh, R. Bedi, B.S. Kaith, Mechanical properties of composite materials based on waste plastic - a review, Mater. Today Proc. 26 (2019) 1293–1301, https://doi.org/10.1016/j.matpr.2020.02.258.
[6] S. Mishra, R.K. Upadhyay, Review on biomass gasification: gasifiers, gasifying mediums, and operational parameters, Mater. Sci. Energy Technol. 4 (2021) 329–340, https://doi.org/10.1016/j.mset.2021.08.009.
[7] J.P. Ciferno, J.J. Marano, Benchmarking Biomass Gasification Technologies for Fuels, Chemicals and Hydrogen Production, US Dep. Energy. Natl. Energy., 2002, p. 58. http://seca.doe.gov/technologies/coalpower/gasification/pubs/pdf/BMassGasFinal.pdf.
[8] M. Kordi, S. Masoud Seyyedi, Biomass gasification systems and different types of gasifiers, effective parameters on gasification process efficiency: an overview, J. Appl. Dyn. Syst. Control. 4 (2021) 1–17.
[9] A. Adil, Brijesh, L. Rao, Integrative approach to kinetic modeling and verification of a downdraft gasification model, Bioresour. Technol. Rep. 25 (2024) 101701, https://doi.org/10.1016/j.biteb.2023.101701.
[10] T. Chmielniak, L. Stepien, M. Sciazko, W. Nowak, Effect of pyrolysis reactions on coal and biomass gasification process, Energies 14 (2021) 1–20, https://doi.org/10.3390/en14165091.
[11] P. Kannan, A. Al Shoaibi, C. Srinivasakannan, Energy recovery from co-gasification of waste polyethylene and polyethylene terephthalate blends, Comput. Fluids 88 (2013) 38–42, https://doi.org/10.1016/j.compfluid.2013.09.004.
[12] M.K. Cohce, I. Dincer, M.A. Rosen, Thermodynamic analysis of hydrogen production from biomass gasification, Int. J. Hydrogen Energy 35 (2010) 4970–4980, https://doi.org/10.1016/j.ijhydene.2009.08.066.
[13] A. Aghaalikhani, J.C. Schmid, D. Borello, J. Fuchs, F. Benedikt, H. Hofbauer, F. Rispoli, U.B. Henriksen, Z. Sárossy, L. Cedola, Detailed modelling of biomass steam gasification in a dual fluidized bed gasifier with temperature variation, Renew. Energy 143 (2019) 703–718, https://doi.org/10.1016/j.renene.2019.05.022.
[14] M.S. Eikeland, R.K. Thapa, B.M. Halvorsen, Aspen Plus Simulation of Biomass Gasification with Known Reaction Kinetic, 2015, pp. 149–156, https://doi.org/10.3384/ecp15119149.
[15] S. Martínez-Lera, J. Pallarés Ranz, On the development of a polyolefin gasification modelling approach, Fuel 197 (2017) 518–527, https://doi.org/10.1016/j.fuel.2017.02.032.
[16] H. Goyal, P. Pepiot, A compact kinetic model for biomass pyrolysis at gasification conditions, Energy Fuel. 31 (2017) 12120–12132, https://doi.org/10.1021/acs.energyfuels.7b01634.
[17] C. Di Blasi, Modeling chemical and physical processes of wood and biomass pyrolysis, Prog. Energy Combust. Sci. 34 (2008) 47–90, https://doi.org/10.1016/j.pecs.2006.12.001.
[18] T.K. Patra, K.R. Nimisha, P.N. Sheth, A comprehensive dynamic model for downdraft gasifier using heat and mass transport coupled with reaction kinetics, Energy. 116 (2016) 1230–1242, https://doi.org/10.1016/j.energy.2016.10.036.
[19] D.A. Nemtsov, A. Zabaniotou, Mathematical modelling and simulation approaches of agricultural residues air gasification in a bubbling fluidized bed reactor, Chem. Eng. J. 143 (2008) 10–31, https://doi.org/10.1016/j.cej.2008.01.023.
[20] J. Qi, Y. Wang, M. Hu, P. Xu, H. Yuan, Y. Chen, A reactor network of biomass gasification process in an updraft gasifier based on the fully kinetic model, Energy. 268 (2023) 126642, https://doi.org/10.1016/j.energy.2023.126642.
[21] D. Cerinski, A.I. Ferreiro, J. Baleta, M. Costa, F. Zimbardi, N. Cerone, J. Wang, Modelling the biomass updraft gasification process using the combination of a pyrolysis kinetic model and a thermodynamic equilibrium model, Energy Rep. 7 (2021) 8051–8061, https://doi.org/10.1016/j.egyr.2021.05.079.
[22] A. Ponzio, S. Kalisz, W. Blasiak, Effect of operating conditions on tar and gas composition in high temperature air/steam gasification (HTAG) of plastic containing waste, Fuel Process. Technol. 87 (2006) 223–233, https://doi.org/10.1016/j.fuproc.2005.08.002.
[23] A. Meng, S. Chen, Y. Long, H. Zhou, Y. Zhang, Q. Li, Pyrolysis and gasification of typical components in wastes with macro-TGA, Waste Manag. 46 (2015) 247–256, https://doi.org/10.1016/j.wasman.2015.08.025.
[24] I. Mporas, P. Kourtessis, A. Al-Habaibeh, A. Asthana, V. Vukovic, J. Senior, Springer Proceedings in Energy Energy and Sustainable Futures Proceedings of 2nd ICESF, 2020 n.d.
[25] Y.A. Crespo, R.A. Naranjo, J.C.V. Burgos, C.G. Sanchez, E.M.S. Sanchez, Thermogravimetric analysis of thermal and kinetic behavior of acacia mangium wood, Wood Fiber Sci. 47 (2015) 9.
[26] J. Sameni, S. Krigstin, M. Sain, Characterization of lignins isolated from industrial residues and their beneficial uses, Bioresources 11 (2016) 8435–8456.
[27] W. Chen, S. Shi, J. Zhang, M. Chen, X. Zhou, Co-pyrolysis of waste newspaper with high-density polyethylene: synergistic effect and oil characterization, Energy Convers. Manag. 112 (2016) 41–48, https://doi.org/10.1016/j.enconman.2016.01.005.
[28] U. Gaur, B. Wunderlich, Heat capacity and other thermodynamic properties of linear macromolecules. II. Polyethylene, J. Phys. Chem. Ref. Data 11 (1982) 313–325, https://doi.org/10.1063/1.555663.
[29] H. Weingrill, W. Hohenauer, K. Resch-Fauster, C. Zauner, Analyzing thermal conductivity of polyethylene-based compounds filled with copper, Macromol. Mater. Eng. 304 (2019) 1–14, https://doi.org/10.1002/mame.201800644.
[30] J.S. Schaul, Polymer processing, Chem. Eng. News 63 (1985) 2.
[31] U. Gaur, B. Wunderlich, Heat capacity and other thermodynamic properties of linear macromolecules. IV. Polypropylene, J. Phys. Chem. Ref. Data 10 (1981) 1051–1064, https://doi.org/10.1063/1.555650.
[32] A. Patti, D. Acierno, Thermal conductivity of polypropylene-based materials, Polypropyl. - Polym. Charact. Mech. Therm. Prop. (2020), https://doi.org/10.5772/intechopen.84477.
[33] S. Lambert, M. Wagner, Microplastics are contaminants of emerging concern in freshwater environments: an overview, in: S. Lambert, M. Wagner (Eds.), Freshw. Microplastics, Springer Open, 2018, p. 302, https://doi.org/10.1007/978-3-319-61615-5.
[34] F. Rouabah, D. Dadache, N. Haddaoui, Thermophysical and mechanical properties of polystyrene: influence of free quenching, ISRN Polym. Sci. 2012 (2012) 1–8, https://doi.org/10.5402/2012/161364.
[35] H.M. Mussa, T.W.M. Salih, Thermal conductivity of wood-plastic composites as insulation panels: theoretical and experimental analysis, J. Silic. Based Compos. Mater. 73 (2021) 54–62, https://doi.org/10.14382/epitoanyag-jsbcm.2021.9.
[36] K. Maeda, Y. Tsunetsugu, K. Miyamoto, T. Shibusawa, Thermal properties of wood measured by the hot-disk method: comparison with thermal properties measured by the steady-state method, J. Wood Sci. 67 (2021) 1–14, https://doi.org/10.1186/s10086-021-01951-1.
[37] M. Tazi, M.S. Sukiman, F. Erchiqui, A. Imad, T. Kanit, Effect of wood fillers on the viscoelastic and thermophysical properties of HDPE-wood composite, Int. J. Polym. Sci. 2016 (2016), https://doi.org/10.1155/2016/9032525.
[38] C. Dupont, R. Chiriac, G. Gauthier, F. Toche, Heat capacity measurements of various biomass types and pyrolysis residues, Fuel 115 (2014) 644–651, https://doi.org/10.1016/j.fuel.2013.07.086.
[39] O.V. Voitkevich, G.J. Kabo, A.V. Blokhin, Y.U. Paulechka, M.V. Shishonok, Thermodynamic properties of plant biomass components. Heat capacity, combustion energy, and gasification equilibria of lignin, J. Chem. Eng. Data 57 (2012) 1903–1909, https://doi.org/10.1021/je2012814.
[40] E. Ranzi, M. Corbetta, F. Manenti, S. Pierucci, Kinetic modeling of the thermal degradation and combustion of biomass, Chem. Eng. Sci. 110 (2014) 2–12, https://doi.org/10.1016/j.ces.2013.08.014.
[41] https://www.engineersedge.com/heat_transfer/thermal_diffusivity_table_13953.htm, (n.d.).
[42] P. Kosky, R. Balmer, W. Keat, G. Wise, Mechanical engineering, in: Explor. Eng., Elsevier, 2021, pp. 317–340, https://doi.org/10.1016/B978-0-12-815073-3.00014-4.
[43] T.M. Ismail, M.A. El-Salam, Numerical and experimental studies on updraft gasifier HTAG, Renew. Energy 78 (2015) 484–497, https://doi.org/10.1016/j.renene.2015.01.032.
[44] X. Gao, L. Lu, M. Shahnam, W.A. Rogers, K. Smith, K. Gaston, D. Robichaud, M. Brennan Pecha, M. Crowley, P.N. Ciesielski, P. Debiagi, T. Faravelli, G. Wiggins, C.E.A. Finney, J.E. Parks, Assessment of a detailed biomass pyrolysis kinetic scheme in multiscale simulations of a single-particle pyrolyzer and a pilot-scale entrained flow pyrolyzer, Chem. Eng. J. 418 (2021), https://doi.org/10.1016/j.cej.2021.129347.
[45] K. Kwiatkowski, K. Bajer, A. Celińska, M. Dudyński, J. Korotko, M. Sosnowska, Pyrolysis and gasification of a thermally thick wood particle - effect of fragmentation, Fuel 132 (2014) 125–134, https://doi.org/10.1016/j.fuel.2014.04.057.
[46] Y. Cao, Y. Bai, J. Du, H2-rich gas production from co-gasification of biomass/plastics blends: a modeling approach, J. Energy Inst. 112 (2024) 101454, https://doi.org/10.1016/j.joei.2023.101454.
[47] Y. Zhou, Experimental and Aspen Plus modeling research on bio-char and syngas co-production by gasification of biomass waste: the products and reaction energy balance evaluation, Biomass Convers. Biorefinery (2023) 5387–5398, https://doi.org/10.1007/s13399-023-04085-0.
[48] Z. Zhao, H. Qin, T. Li, B. Hua, Y. Hou, T. Chen, H. Ström, CFD simulation of soot generation during biomass gasification in a cyclone gasifier, Fuel 364 (2024), https://doi.org/10.1016/j.fuel.2024.131103.
[49] N. Raza, M. Ahsan, Influence of distributor plate design on mixing characteristics of rice husk biomass in a bubbling fluidized bed gasifier: an experimental and CFD study, Fuel 358 (2024) 129893, https://doi.org/10.1016/j.fuel.2023.129893.
[50] N. Samani, R. Khalil, M. Seljeskog, J. Bakken, R.K. Thapa, M.S. Eikeland, Experimental and simulation studies of oxygen-blown, steam-injected, entrained flow gasification of lignin, Fuel 362 (2024), https://doi.org/10.1016/j.fuel.2023.130713.
[51] L.L. Berkel, P. Debiagi, H. Nicolai, M.A. Amjed, A. Stagni, C. Hasse, T. Faravelli, Development of a multiphase chemical reactor network method as a tool for simulating biomass gasification in fluidized beds, Fuel 357 (2024) 129731, https://doi.org/10.1016/j.fuel.2023.129731.
[52] M.Y. Arshad, H. Jaffer, M.W. Tahir, A. Mehmood, A. Saeed, Maximizing hydrogen-rich syngas production from rubber wood biomass in an updraft fluidized bed gasifier: an advanced 3D simulation study, J. Taiwan Inst. Chem. Eng. 156 (2024) 105365, https://doi.org/10.1016/j.jtice.2024.105365.